Stimulated nuclear translocation of NF-κB and shuttling differentially depend on dynein and the dynactin complex

Cynthia K. Shrum[a], Daniel DeFrancisco[b], and Mollie K. Meffert[a,c,1]

Departments of [a]Biological Chemistry and [c]Neuroscience, The Johns Hopkins University School of Medicine, 725 N. Wolfe St., Baltimore, MD 21205; and [b]The Johns Hopkins University, 3400 N. Charles St., Baltimore, MD 21218

Translocation from the cytoplasm to the nucleus is required for the regulation of gene expression by transcription factors of the nuclear factor kappa B (NF-κB) family. The p65:p50 NF-κB heterodimer that predominates in many cell types can undergo stimulated movement, following degradation of the IκB inhibitor, as well as shuttling in the absence of stimulation with IκB bound. Disruption of the dynactin complex and knockdown of endogenous dynein were used to investigate the nuclear translocation requirements for stimulated and shuttling movement of NF-κB. A differential dependence of these two modes of transport on the dynein molecular motor and dynactin was found. NF-κB used active dynein-dependent transport following stimulation while translocation during shuttling was mediated by a dynein-independent pathway that could be potentiated by dynactin disruption, consistent with a process of facilitated diffusion. Nuclear translocation and activation of NF-κB-dependent gene expression showed a dependence on endogenous dynein in a variety of cell types and in response to diverse activating stimuli, suggesting that dynein-dependent transport of NF-κB may be a conserved mechanism in the NF-κB activation pathway and could represent a potential point of regulation.

NF-kappaB | nuclear transport | transcription | molecular motor | active transport

The NF-κB or Rel transcription factors are ubiquitously-expressed regulators of gene expression that are essential for physiological processes ranging from innate and adaptive immunity to learning and memory. NF-κB functions as a dimer and is retained in a latent form in the cytoplasm, bound to the inhibitor of NF-κB (IκB). In the canonical pathway, incoming stimuli trigger activation of the IκB-kinase complex (IKK) that phosphorylates IκBα and leads to its degradation. The subsequent translocation of active IκB-free NF-κB from cytoplasm to nucleus is critical for NF-κB-dependent gene expression. In the absence of IκB degradation, NF-κB can undergo stimulus-independent movement back and forth between the nucleus and cytoplasm in a process termed shuttling (1). Shuttling of p65:p50 NF-κB dimers is believed to result from incomplete masking of the p50 nuclear localization sequence (NLS) by bound IκBα and can be observed by blocking exportin1/crm1-mediated nuclear export under unstimulated conditions (2).

While NF-κB requires importin family members to cross the nuclear pore (3), the molecular mechanisms underlying NF-κB cytoplasmic movement remain poorly understood. Studies examining the role of microtubules are conflicting, possibly because the pharmacological agents that disrupt microtubules result in a confounding activation of NF-κB (4–10). Microtubule-dependent transport can also be probed by disrupting the multisubunit dynactin complex, and it was recently reported that dynactin could play a role in the nuclear accumulation of neuronal NF-κB (10). Dynactin regulates the processivity of molecular motors using microtubules, including cytoplasmic dynein and kinesin

(11, 12). Dynein is a retrograde motor, mediating minus-end directed movement on microtubules. Kinesin has multiple family members, most of which mediate anterograde, but some of which also mediate retrograde movement (13, 14). Potential roles for dynactin in nonmotile processes have also been recognized (15–19). This study tested the role of dynactin and dynein on the rate and amplitude of NF-κB nuclear translocation under conditions of shuttling and in multiple activation paradigms. The finding of differential roles for dynactin and dynein in shuttling and stimulated translocation suggests that NF-κB can use multiple mechanisms for cytoplasmic transport.

Results

Disruption of Dynactin Function in MEFs Leads to Dose-Dependent Inhibition of NF-κB Nuclear Translocation. The dynactin complex is disrupted by overexpression of either the p50/dynamitin subunit or of the first coiled coil domain (CC1) of the largest dynactin subunit, p150Glued. Dynactin function is required for the lamellar conformation and function of the Golgi apparatus. Overexpression in wild-type murine embryonic fibroblasts (MEFs) of CC1 tagged with monomeric red fluorescent protein (RFP-CC1) or of dynamitin tagged with the mCherry fluorophore (C-dynamitin) resulted in Golgi condensation or dispersal, respectively, [supporting information (SI) Fig. S1] demonstrating that fluorophore tagged RFP-CC1 and C-dynamitin retain dynactin inhibition. Stimulus-dependent NF-κB translocation can be monitored in living cells expressing a green fluorescent protein-tagged p65 (GFPp65) subunit of NF-κB (20). Robust GFPp65 nuclear translocation in response to TNFα was observed by time-lapse confocal imaging of MEFs coexpressing mCherry (Fig. 1A and B). Evaluation of a nuclear region of interest (ROI) from confocal slices was used to quantitate the time course of GFPp65 nuclear accumulation. Binning of cells according to expression level of RFP-CC1 or C-dynamitin, using absolute fluorescence units (fu) with confocal laser power, voltage, and gain held constant throughout experiments, revealed dose-dependent reduction in the rate and amplitude of TNFα-stimulated nuclear GFPp65 accumulation by dynactin disruption (Fig. 1 A and B). At high expression levels of RFP-CC1 or C-dynamitin (fu > 600), GFPp65 nuclear translocation was undetectable.

Dynactin Disruption Specifically Inhibits Induced NF-κB-Dependent Transcription. The effect of dynactin disruption on NF-κB-dependent gene expression was tested by NF-κB luciferase
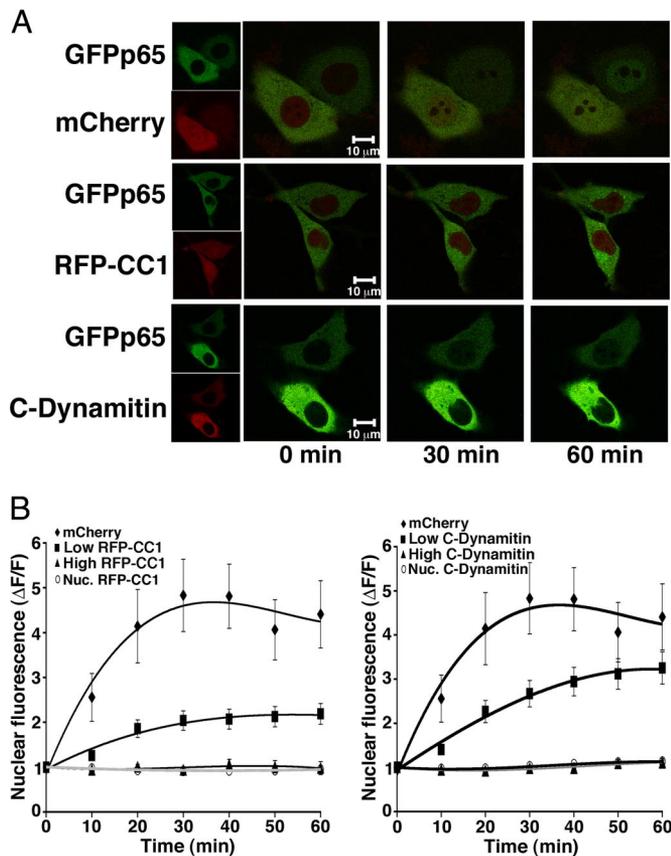
CELL BIOLOGY

Fig. 1. Dynactin Disruption Reduces the Rate and Amplitude of Stimulated NF-κB Nuclear Translocation. (*A*) Representative confocal projections from the time course of GFPp65 nuclear translocation in live MEFs coexpressing either soluble mCherry, or RFP-CC1, or C-Dynamitin. Green and red channels are overlayed in the large panels; small panels (*Left*) show each channel separately. Nuclear accumulation of GFPp65 following application of TNFα (time 0) is evident by 30 min in cells expressing mCherry, but not RFP-CC1 or C-Dynamitin. (*B*) The calculated change in nuclear GFPp65 fluorescence for each time point is averaged across all experiments for MEFs expressing RFP-CC1 (*Left*), C-Dynamitin (*Right*), or mCherry; a level of one is no change. Cells are binned according to high (>600 fu) or low (<600 fu) expression of RFP-CC1 and C-Dynamitin to show dose-dependence. Both high and low RFP-CC1 expressors are significantly different from control (mCherry) at all time points ≥20 min ($n = 12$–34 cells for each graphed point, $P \leq 0.05$). High C-Dynamitin expressers are significantly different from control (mCherry) at all points ≥20 min ($n = 10$–34 cells each point, $P \leq 0.05$), and low C-Dynamitin expressors are significantly different from control (mCherry) at time points 10–40 min ($n = 12 - 34$ cells for each point, $P \leq 0.05$). ΔF/F for nuclear RFP (Nuc.RFP-CC1) and C-Dynamitin (Nuc. C-Dynamitin) does not change over time and provides a measure of cell health and nuclear integrity. Error bars represent one s.e.m.

reporter assay. Dynactin disruption with increasing amounts of C-dynamitin resulted in dose-dependent inhibition of TNFα-induced NF-κB-dependent gene expression (Fig. 2*A*). Fold induction of the NF-κB reporter by TNFα was inhibited without significant effects on unstimulated reporter activity. Dynactin disruption does not globally inhibit transcription since the activity of an NF-κB-independent reporter in which the consensus κB sites were mutated (mutκB) (21) was not significantly altered (Fig. 2*A*).

To assess whether dynactin might be generally required by other transcription factors, we tested the effects of dynactin disruption on a cyclic-AMP response element-binding (CREB)-dependent reporter (CRE luciferase) and on a reporter responsive to the nuclear factor of activated T-cells (NFAT) transcription factor (NFAT luciferase). While CREB is located primarily
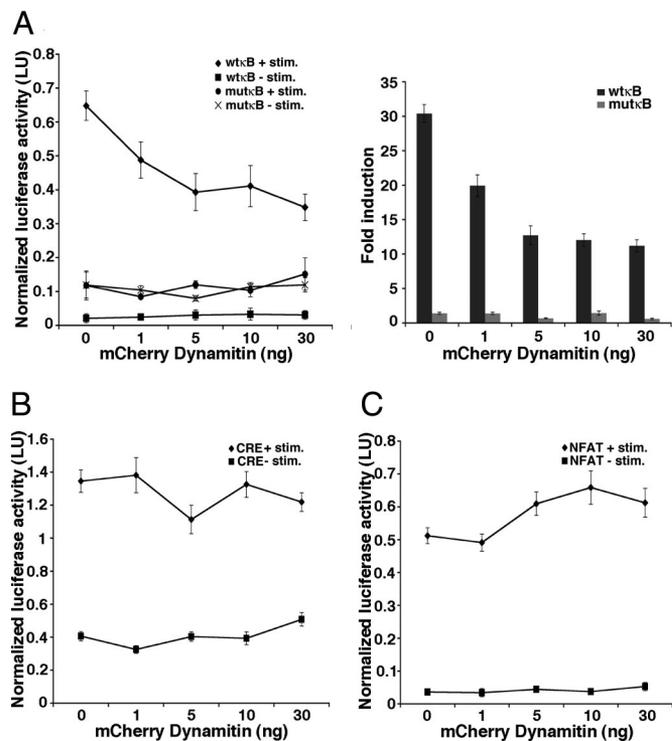

Fig. 2. Specificity of Dynactin Disruption for NF-κB. (*A*) The effect of dynactin disruption on NF-κB-dependent gene expression is tested by TNFα stimulation of 293T cells coexpressing wild-type (wtκB) or mutant (mutκB) NF-κB reporters and increasing amounts of C-Dynamitin. Dose-dependent inhibition of wtκB reporter activity is evident both by normalized luciferase activity (*Left*) and by calculated fold induction relative to unstimulated samples (*Right*). Inhibition of wtκB reporter activity by increasing C-Dynamitin plateaus between 10–30 ng transfected DNA and is significantly different from cells not expressing C-Dynamitin (0 ng, $n = 5$–6 samples each point, $P \leq 0.001$) at all tested doses. Activity of a reporter not dependent on NF-κB (mutκB) is unaffected by TNFα or by C-Dynamitin expression. (*B*) The effect of dynactin disruption on CREB-dependent gene expression in 293T cells cotransfected with CREB reporter and increasing amounts of C-Dynamitin in the presence or absence of forskolin and ionomycin stimulation. Stimulated CREB activity (CRE + stim.) is not significantly altered by increasing amounts of transfected C-Dynamitin; basal CREB activity (CRE − stim.) shows a nonstatistically significant elevation at 30 ng transfected C-Dynamitin ($n = 6$ samples each point). (*C*) The effect of dynactin disruption on NFAT activation in 293T cells cotransfected with NFAT reporter and increasing amounts of C-Dynamitin in the presence or absence of thapsigargin and PMA stimulation. Stimulated NFAT activity is not inhibited by dynactin disruption and shows a nonstatistically significant elevation at higher transfected C-Dynamitin levels; C-Dynamitin overexpression does not alter basal NFAT activity ($n = 6$ samples each point). Error bars represent one s.e.m.

in the nucleus, NFAT is initially cytoplasmic and requires stimulus-induced nuclear relocalization for activation. Stimulus-induced activation of CREB or of NFAT was not inhibited by dynactin disruption (Fig. 2 *B* and *C*). Slightly elevated NFAT activity in the presence of stimulation and elevated basal CREB activity in the absence of stimulation were observed at high C-dynamitin concentrations, but these effects did not reach significance (Fig. 2 *B* and *C*). These results suggest that even among transcription factors requiring nuclear translocation for activation, such as NFAT and NF-κB, distinct transport mechanisms exist.

Disruption of Dynactin Function Enhances the Rate and Amplitude of NF-κB Trafficking by Shuttling. The effect of dynactin disruption on unstimulated shuttling of NF-κB-IκBα complexes was studied by treating cells with leptomycin B (LMB) to block CRM1/
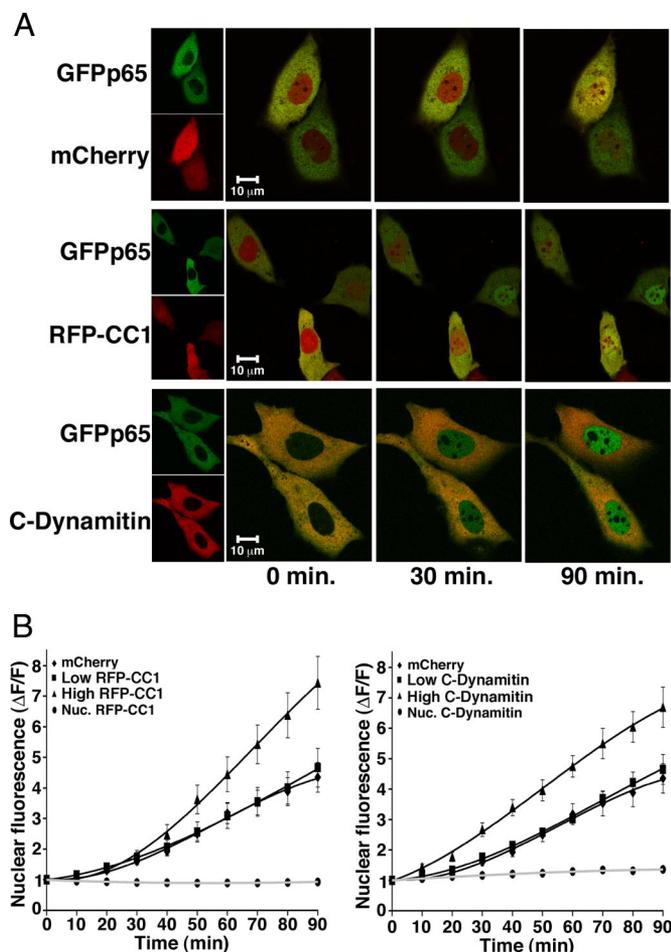
Fig. 3. Loss of Dynactin Function Enhances Shuttling of NF-κB. (*A*) Representative confocal projections of live MEFs expressing GFPp65 and either mCherry, RFP-CC1, or C-Dynamitin in a time course from 0 to 90 min following leptomycin B addition (time 0) to examine NF-κB shuttling. Small panels (*Left*) show separate green and red channels, large panels (*Right*) are overlayed. (*B*) The quantitated change in nuclear GFPp65 fluorescence at each time point is averaged across all experiments for MEFs expressing mCherry, RFP-CC1 (*Left*), or C-Dynamitin (*Right*). Based on average fluorescence, cells are binned into high (> 300 fu) or low (< 300 fu) expression for RFP-CC1 and C-Dynamitin. The rate and amplitude of GFPp65 nuclear accumulation by shuttling does not significantly differ from control at low levels of RFP-CC1 or C-Dynamitin. High expression of RFP-C1 or C-Dynamitin significantly enhance rate and amplitude of GFPp65 shuttling for time points ≥50 min or ≥30 min, respectively (RFP-CC1: $n = 12 - 19$ cells, $P \leq 0.05$; C-Dynamitin: $n = 16 - 21$ cells, $P \leq 0.01$ for each time point). Error bars represent one s.e.m.

exportin1-mediated nuclear export (2). Representative projections from time-lapse confocal imaging of LMB-treated MEFs expressing GFPp65 and either mCherry, RFP-CC1, or C-dynamitin are shown in Fig. 3*A*. Quantitation of nuclear GFPp65 (Fig. 3*B*) shows that, in contrast to its effects on stimulated movement, dynactin disruption did not inhibit nuclear NF-κB translocation by shuttling. Instead, both RFP-CC1 and C-dynamitin elicited a dose-dependent increase in the rate of GFPp65 nuclear shuttling in comparison to cells expressing mCherry alone. Dynactin disruption by C-dynamitin expression similarly enhanced the nuclear translocation of endogenous p65 as assessed by immunofluorescence (data not shown). The nuclear levels of RFP-CC1, C-dynamitin, and mCherry were unaffected by LMB (Fig. 3*B*). Analysis of GFPp65 nuclear accumulation longer than 90 min following LMB exposure was hampered by loss of cell viability, as assessed by visual inspection

and the eventual nuclear accumulation of untagged fluorophore (mCherry). Analysis of a limited number of healthy long-term LMB treated cells indicated that increased nuclear GFPp65 in high RFP-CC1 and C-dynamitin expressing cells reached plateau after 90 min (data not shown).

Loss of Endogenous Dynein Function Inhibits Stimulus-Induced NF-κB Activation in Multiple Cell Types. Dynactin can regulate the processivity of multiple molecular motors and dynactin disruption can disable both anterograde and retrograde trafficking (11, 12); in addition, dynactin may act as a scaffold to dock anchoring or signaling proteins independently of its role in cellular transport (15–19). To directly assess the role of cytoplasmic dynein in the NF-κB response to diverse activating stimuli in multiple cell types, we designed shRNAs against the heavy chain of dynein for both mouse and human species. The dynein heavy chain (DHC) was targeted because, unlike the light and intermediate chains, there is only one known heavy chain isoform of nonflagellar cytoplasmic dynein (DYNC1H1). DHC contains ATPase activity and is essential to dynein's capacity to move cargo along microtubules. shRNAs targeting murine (shDHC1,shDHC2) or human (shDHC1) DHC, and a nontargeting mutant of shDHC1 (shMUT) were inserted into a pLK0.1 lentiviral vector modified to coexpress GFP. Infection of MEFs and 293T cells produced dose-dependent knockdown of endogenous DHC by virus expressing targeting but not mutant shRNA (Fig. 4*A*). To test the effect of dynein knockdown on NF-κB nuclear translocation, MEFs were infected for 3 days with virus expressing shDHC1 or shMUT. On day 2 of infection, MEFs were transfected with an mCherry tagged p65 subunit of NF-κB (mCherryp65), and subjected to TNFα stimulation and time-lapse confocal imaging (Fig. 4 *B* and *C*) the following day. Dynein knockdown significantly inhibited mCherryp65 nuclear translocation at time points ≥20 min after TNFα (Fig. 4 *B* and *C*; see Fig. S2 and *SI Methods* for similar results with endogenous p65). The effect of dynein knockdown on NF-κB-dependent gene expression was examined by reporter assays in distinct cellular settings. NF-κB reporter assays in TNFα-stimulated MEFs (Fig. 4*D*, *Left*) and 293T cells (Fig. 4*D*, *Right*) showed dose-dependent inhibition of stimulated NF-κB-dependent transcription in cells expressing shDHC1 and shDHC2, but not shMUT.

To test dynein's role in other cellular settings requiring NF-κB function, we evaluated NF-κB activation from both the immunological synapse and the neuronal synapse (Fig. 4*E*). Engagement of the T cell receptor (TCR) by the major histocompatibility complex (MHC) class II of an antigen-presenting B cell initiates the formation on T cells of an ordered membrane-associated signaling complex called the immunological synapse. Signaling through the immunological synapse is essential for T cell activation and induces multiple transcription factors, including NF-κB. To study this activation pathway, Jurkat T cells were infected with shDHC1 or shMUT expressing lentivirus at high MOI. 12 h postinfection Jurkat T cells were transfected for NF-κB reporter assay and allowed to express for 40 h before coincubation with Raji B cells presenting the *staphylococcal* enterotoxin E (SEE) superantigen to initiate immunological synapse formation (see *Methods*) (22). Immunological synapse formation induced robust NF-κB reporter activation, relative to unstimulated cells, in T cells expressing no shRNA or shMUT. In contrast, Jurkat T cells expressing shDHC1 showed significantly reduced NF-κB activation relative to no shRNA or shMUT-expressing cells (Fig. 4*E*, *Left*); mutκB reporter activity was unaltered by shDHC1 compared to no shRNA or shMUT.

NF-κB activation by excitatory neurotransmission occurs in multiple brain regions and may participate in NF-κB function in learning and memory. To test the role of dynein in neurotransmission-induced NF-κB activation, primary hippocampal neuronal cultures were exposed to a GABA_A receptor antagonist
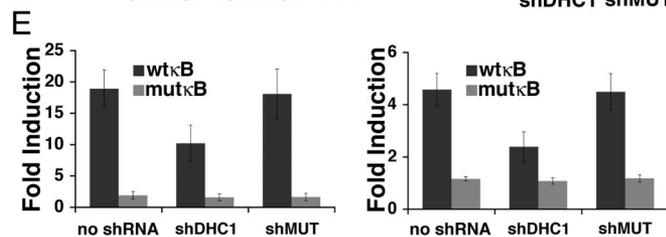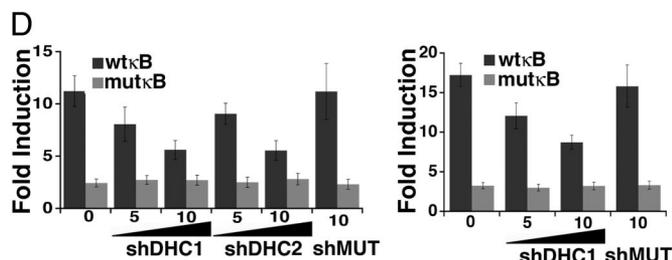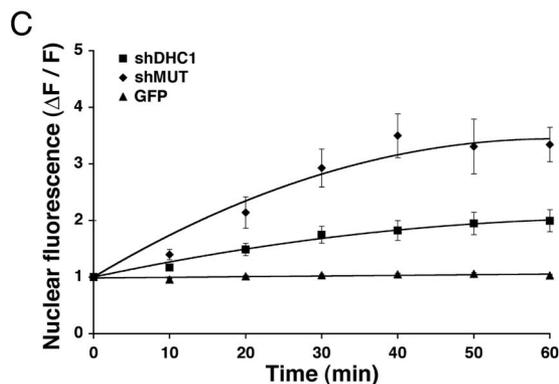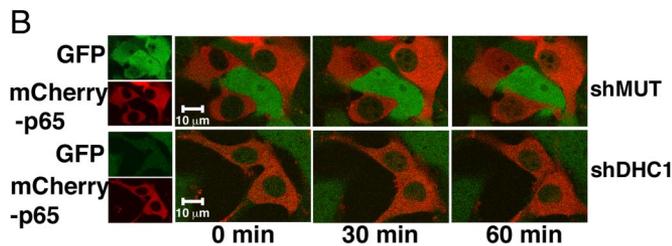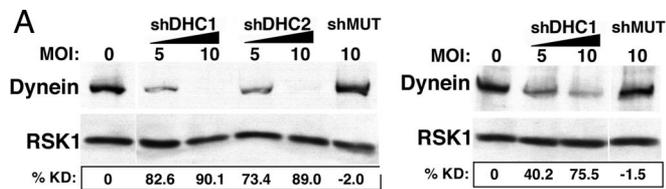
Fig. 4. Dynein is Required for the NF-κB Transcriptional Response to Diverse Stimuli in Multiple Cellular Settings. (*A*) shRNA-mediated dynein knockdown is verified by immunoblot with anti-DHC antibody of lysates from MEFs (*Left*) or 293T cells (*Right*). Increasing MOI results in dose-dependent reduction in DHC for shDHC1 and shDHC2, but not shMUT, as quantified by percent DHC knockdown (%KD). Samples were normalized for total protein before gel loading; anti-RSK1 serves as loading control. (*B*) Representative confocal projections of TNFα-stimulated nuclear translocation of mCherryp65 in MEFs infected with lentivirus expressing shDHC1 or shMUT. Overlayed images (*Right*) show inhibition of stimulated mCherryp65 nuclear accumulation at 30 and 60 min in cells expressing shDHC1 relative to shMUT. (*C*) Quantitated change in nuclear fluorescence demonstrates significant inhibition of TNFα-stimulated mCherryp65 nuclear accumulation in MEFs expressing shDHC1 compared to shMUT at all time points ≥20 min (*n* = 12–16 cells for each point, *P* ≤ 0.005), while nuclear levels of untagged GFP are unchanged. (*D*) Average fold induction from reporter assays with wild-type (wtκB) or mutant (mutκB) NF-κB reporters in TNFα-stimulated MEFs (*Left*) or 293T cells (*Right*) 3 days after infection with the indicated MOI of virus expressing shDHC1, shDHC2, or
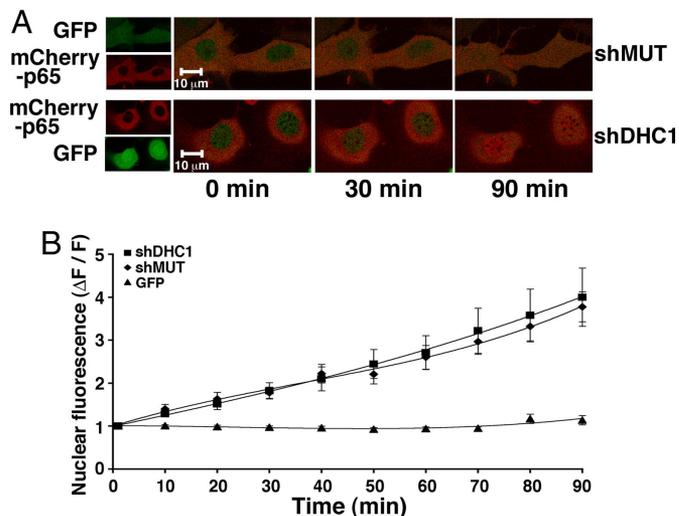

Fig. 5. Shuttling of NF-κB is Not Altered by Loss of Dynein. (*A*) Representative confocal projections show no difference in mCherryp65 nuclear accumulation in LMB-treated (time 0) MEFs 3 days after infection with lentivirus expressing shMUT or shDHC1. (*B*) Average change in nuclear mCherryp65 fluorescence in LMB-treated MEFs 3 days after infection does not differ between shDHC1 or shMUT expressing cells. Nuclear levels of untagged GFP, also produced by pLK0.1 infection, are unchanged by LMB. Error bars represent one s.e.m.

(Bicuculline) that reduces endogenous inhibition and enhances excitatory neurotransmission (20). Bicuculline effectively induced NF-κB reporter activity relative to unstimulated cells in neuronal cultures expressing no shRNA or shMUT, while shDHC1-expressing cultures had significantly reduced bicuculline-stimulated NF-κB activation (Fig. 4*E*, *Right*). MutκB reporter activity was unaffected by shDHC1, demonstrating some specificity for NF-κB-dependent gene expression and an absence of effects on general transcription machinery. Collectively, these experiments show that the full induction of NF-κB-dependent gene expression from both neuronal and immunological synapses relies upon dynein function.

Loss of Endogenous Dynein Function Does Not Alter Nonstimulated Transport of NF-κB by Shuttling. To test whether shuttling enhancement by dynactin disruption (Fig. 3) reflects either a requirement for the dynein motor or an alternative dynactin function, the effect of dynein knockdown was examined. MEFs were infected at high MOI with either shDHC1 or shMUT, followed by mCherryp65 transfection 2 days later, and time-lapse confocal imaging 24 h posttransfection in the presence of LMB to capture shuttling (Fig. 5, or Fig. S3 for endogenous p65). Representative images (Fig. 5*A*) and quantitation of nuclear ROI (Fig. 5*B*) demonstrate that dynein knockdown did not significantly alter the rate or amplitude of NF-κB shuttling. Nuclear accumulation of the untagged GFP fluorophore coexpressed with shRNA did not occur, providing a measure of nuclear integrity. The amplitude and time course of NF-κB nuclear accumulation by shuttling in cells expressing shDHC1 or shMUT (Fig. 5) did not

shMUT. Differences in fold induction relative to no infection or shMUT are significant at all MOI for both shDHC1 and shDHC2 (*n* = 5–6 samples each point, *P* ≤ 0.05). (*E*) Assays with wtkB or mutκB reporters in jurkat T cells (*Left*) or primary hippocampal neurons (*Right*) 3 days after infection with the indicated MOI of virus expressing shDHC1, shDHC2, or shMUT. Fold induction in Jurkat T cells activated by T cell receptor stimulation or primary neurons activated by synaptic stimulation is significantly different between shDHC1 and no shRNA or shMUT (*n* = 6 samples each, *P* ≤ 0.05). Error bars represent one s.e.m.

statistically differ from cells expressing mCherry alone (Fig. 3, $P \leq 0.05$). These results suggest that enhancement of NF-κB shuttling by dynactin disruption (Fig. 3) is independent of dynactin's role in regulating dynein processivity.

Discussion

Our findings indicate that stimulated nuclear translocation of activated NF-κB and nuclear translocation of NF-κB by shuttling use distinct transport mechanisms. These findings were replicated in live cell imaging of exogenous GFPp65 and by immunocytochemistry for endogenous p65. Loss of the dynein motor or disruption of dynactin both strongly inhibited stimulated nuclear translocation of NF-κB and the induction of NF-κB-dependent gene expression. In contrast, dynein appeared to play no role in shuttling of NF-κB and dynactin disruption resulted in *enhanced* shuttling. A potential unifying model is that NF-κB may undergo active transport using dynein following stimulation, while shuttling may be diffusion-mediated. If shuttling is diffusion-mediated, enhancement of the process by dynactin disruption could be consistent with emerging roles for dynactin in nonmotile processes such as tethering of signaling molecules (15–19).

We previously found that neuronal NF-κB moved more rapidly in a retrograde than anterograde direction from distal dendrites following synaptic stimulation (20). While diffusion could mediate this effect (e.g., in the context of a binding-protein gradient), the finding suggested that stimulated NF-κB might use active transport. Brain NF-κB has been reported to coimmunoprecipitate dynein intermediate chain and components of dynactin in the presence of cross-linkers (10), and dynein is also concentrated at the postsynaptic density in neurons (23) and recruited to the immunological synapse in T cells (24), both sites which can signal NF-κB activation. We have now shown that NF-κB nuclear transport following stimulation depends upon the dynein molecular motor. A conserved dynein requirement for the full induction of NF-κB-dependent gene expression was found in all tested mammalian cells (MEFs, 293T, Jurkat, and primary neuronal cultures) and in response to diverse stimulation paradigms (TNFα, immunological synapse formation, and neuronal synaptic activation), indicating that dynein-mediated transport of activated NF-κB is likely characteristic rather than an exception. While effects were robust and significant, dynein knockdown did not generate a complete block of NF-κB-dependent gene expression in any tested cell type. Several possibilities could account for a lack of complete inhibition by reporter assay, including incomplete or heterogeneous dynein-knockdown in the cell populations, or residual stimulated nuclear transport in the absence of dynein function. In dynein-knockdown imaging experiments evaluating individual cells, residual TNFα-induced nuclear transport was also observed, but the remaining dynein level in each cell is unknown. In contrast, in dynactin-disruption experiments, where cells could be binned by expression level of C-dynamitin or RFP-CC1, a complete inhibition of nuclear transport of NF-κB was achieved in high-expressing cells. Dynactin disruption is reported to be graded by expression levels of the disrupting component (e.g., dynamitin or CC1) (25). Taken together, our results support an essential role for dynein-dependent active transport in the rapid NF-κB response to inducing stimuli.

While microtubule-dependent transport of vesicles and other large cargo has been well studied, several reports have highlighted microtubule-dependent transport of small nonvesicular cargo and have also linked dynactin and dynein to nonvesicular protein transport (26–29). A microinjected complex of the p50 NF-κB subunit with plasmid DNA was reported to enhance nuclear import and cytoplasmic migration of the DNA with a dependence on microtubules, dynein, and the p50 NLS (30); sequences distinct from a NLS bind dynein, and the presence of an NLS can, but does not necessarily, confer microtubule-dependent transport (29). Consensus sequences conferring interaction with the dynein light chains LC8 and Tctex-1 are beginning to be defined. Our analysis of human and mouse p65 protein indicate that no known sites appear present; however, the interaction sites of most dynein cargo remain uncharacterized (29, 31).

Numerous signaling molecules, including other transcription factors, use movement from cytoplasm to nucleus as a regulatory mechanism. The specificity of NF-κB's requirement for dynein-based transport was tested by examining the effect of loss of endogenous dynein on the activity of two additional transcription factors, one which is largely localized in the nucleus (CREB) and another which undergoes cytoplasmic to nuclear translocation (NFAT). Interestingly, dynein knockdown did not significantly alter either CREB or NFAT reporter activity, although it has been reported that perturbations in the microtubule network could inhibit NFAT (32). While p53 is known to use dynein (26), the transport mechanisms of many nuclear localizing molecules are either unknown or are independent of the cytoskeleton (29, 33, 34). The further understanding of both dynein-dependent and independent mechanisms of NF-κB transport may reveal additional regulatory points in this widespread signaling pathway.

Methods

Cells and Constructs. MEFs were maintained in Dulbecco Modified Eagle's medium (DMEM) supplemented with 10% calf serum and the human embryonic kidney 293T cell line in DMEM with 10% FBS (FBS). The human Raji B and Jurkat T cell lines were maintained in RPMI 1640 with 10% FBS and 50 μM β-mercaptoethanol. Murine hippocampal neurons were cultured as previously described (20).

The GFPp65 construct was previously described (20). To produce mCherryp65, mCherry (gift of R. Tsien, La Jolla, CA) was inserted into the C1 expression vector (Clontech) to create an N-terminal p65 fusion (mCherryp65). Dynamitin and RFP-CC1 were gifts of T. Schroer (Baltimore, MD). mCherry fused to the N terminus of Dynamitin was made by subcloning dynamitin into mCherry-C1 vector.

shRNA constructs were prepared by cloning shRNAs into the lentiviral vector pLKO.1. pLKO.1 was modified by excision of the puromycin resistance cassette and insertion of EGFP in its place (pLKO.1GFP, J. Pomerantz, Baltimore, MD). The following sequences were used to produce shRNA: shDHC1: 5'GCTAAACTTGGAACGTGCGTT3', shDHC2: 5'GGCGTTTCCAGCATCATCTTA3', shMUT: 5'GCCAACCTCGGTACATGAGTA3'. shDHC1 targets both mouse and human DHC; shDHC2 targets the mouse sequence only. shMUT contains 7 mismatches with shDHC1. shDHC1, shDHC2, and shMUT sequences were subjected to blast search to ensure lack of significant complementarity for off-target mRNAs.

Dynein Knockdown by siRNA. Lentiviral particles were prepared as previously described (35). Lentiviral infection was performed 3–4 days before assessment by immunoblot or functional assay to allow time for effective siRNA. Immunoblots of lysates from infected cells were probed with anti-DHC antibody (1:200, Santa Cruz Biotechnology, 9115) and a loading control anti-p90 ribosomal protein S6 kinase (RSK1, Epitomics, 2004–1) antibody. DHC and RSK1 levels were quantitated by densitometry and knockdown efficiency calculated by first normalizing DHC to RSK1 for each sample and then dividing by the normalized value for MOI of 0.

Reporter Assays. NF-κB-dependent transcription was assayed by transient transfection of an NF-κB luciferase reporter (Igκ_2-IFN-LUC) containing two copies of the Ig light chain κB-site or a mutant reporter with four residues of the NF-κB consensus binding site mutated as previously described (21). Transcription regulated by NFAT or CREB was assayed by transient transfection of NFAT-responsive or CRE-luciferase reporters, respectively (Clontech). In all reporter assays, cotransfection of the pCSK-lacZ vector, which constitutively expresses β-galactosidase and is not regulated by NF-κB, NFAT, or CREB, served to normalize transfection efficiency and extract recovery for each sample. Each reporter experiment included extracts from cells transfected with pcDNA3 alone as a reference control. Cell lysates were prepared using 1X lysis buffer (reporter lysis buffer, Promega) and luciferase (Promega) and chemiluminescent β-gal (Roche) reporter assays were conducted 46 h after transfection and 3–4 h after stimulation according to manufacturer instructions using a luminometer (Perkin–Elmer). Samples were compared by subtracting

the background activity of the reference control, and then normalizing the luciferase activity of each sample to its β-gal activity. Fold induction was calculated by dividing normalized stimulated samples by normalized unstimulated samples.

Stimulation of 293T (transfected by CaPO$_4$) and MEFs (transfected by TransIT-LT1 Reagent, Mirus Bio) was conducted by bath application of either human TNFα (25 ng/ml) for the NF-κB reporter, thapsigargin (1 μM) and phorbol 12-myristate 13-acetate (PMA, 50 nM) for the NFAT reporter, or forskolin (10 μM) and ionomycin (2 μM) for the CREB reporter. NF-κB was activated in primary hippocampal cultures (transfected by Lipofectamine 2000, Invitrogen) by synaptic stimulation using bicuculline (50 μM) as described (20). Antigen-presenting Raji cells were prepared by incubation with the superantigen SEE (0.4 ng/ml) for 30 min at 37 °C. Jurkats were transfected (Fugene 6, Roche) for reporter assay immediately following lentiviral infection with shDHC1 or shMUT. 40 h posttransfection, Jurkats were stimulated through the T cell receptor by incubation with the SEE-presenting Raji B cells for 4 h before harvest for reporter assay (J. Pomerantz, unpublished techniques).

Microscopy. MEFs were cotransfected with desired constructs 24–48 h before live confocal imaging at 37 °C in Tyrode's buffer (in mM) [119 NaCl, 4.5 KCl, 2 CaCl$_2$, 0.5 MgCl$_2$, 25 Glucose, 10 Hepes (pH7.33), .01 Glycine] on an LSM5 Pascal with Axiovert 200 (Carl Zeiss). When required, lentiviral infection occurred 24 h before transfection, followed by imaging 48 h posttransfection. For time

course experiments, confocal images were acquired as a z stack of three slices, ranging from 0.3–0.7 μm, to minimize phototoxicity. EGFP was excited at 488 nm and emissions collected at 505–530 nm; RFP and mCherry were excited at 543 nm and emissions collected above 560 nm. Laser power, detector gain, and offset were adjusted to keep fluorescence signals within the dynamic range; images were never saturated. To permit binning by absolute fluorescence for C-Dynamitin and RFPCC1, laser power, gain, and offset were held constant across all experiments. RFPCC1 was binned by nuclear ROI while C-Dynamitin, which is nonnuclear, was binned by cytoplasmic ROI. Following 24 h serum starvation (0.5% calf serum), cells were treated with hTNFα (25 ng/ml) or leptomycin B (LMB, 25 nM) and imaged every 10 min for 60 or 90 min, respectively, including a pretreatment image (t = 0). Nuclear or cytoplasmic fluorescence was quantitated by ROI analysis (Pascal, Zeiss). Nuclear ROI was measured in a representative area not including nucleoli. Normalized change in nuclear fluorescence was calculated by: (fluorescence–fluorescence$_{initial}$)/fluorescence$_{initial}$, where fluorescence$_{initial}$ was determined from the pretreatment time point.

Statistical comparisons were made by unpaired two-tailed t tests.

1. Huang TT, Kudo N, Yoshida M, Miyamoto S (2000) A nuclear export signal in the N-terminal regulatory domain of IkappaBalpha controls cytoplasmic localization of inactive NF-kappaB/IkappaBalpha complexes. *Proc Natl Acad Sci USA* 97:1014–1019.
2. Tam WF, Lee LH, Davis L, Sen R (2000) Cytoplasmic sequestration of rel proteins by IkappaBalpha requires CRM1-dependent nuclear export. *Mol Cell Biol* 20:2269–2284.
3. Fagerlund R, Kinnunen L, Kohler M, Julkunen I, Melen K (2005) NF-{kappa}B is transported into the nucleus by importin {alpha}3 and importin {alpha}4. *J Biol Chem* 280:15942–15951.
4. Rosette C, Karin M (1995) Cytoskeletal control of gene expression: depolymerization of microtubules activates NF-kappa B. *J Cell Biol* 128:1111–1119.
5. Spencer W, *et al.* (1999) Taxol selectively blocks microtubule dependent NF-kappaB activation by phorbol ester via inhibition of IkappaBalpha phosphorylation and degradation. *Oncogene* 18:495–505.
6. Bourgarel-Rey V, *et al.* (2001) Involvement of nuclear factor kappaB in c-Myc induction by tubulin polymerization inhibitors. *Mol Pharmacol* 59:1165–1170.
7. Mistry P, Deacon K, Mistry S, Blank J, Patel R (2004) NF-kappaB promotes survival during mitotic cell cycle arrest. *J Biol Chem* 279:1482–1490.
8. Mikenberg I, Widera D, Kaus A, Kaltschmidt B, Kaltschmidt C (2006) TNF-alpha mediated transport of NF-kappaB to the nucleus is independent of the cytoskeleton-based transport system in non-neuronal cells. *Eur J Cell Biol* 85:529–536.
9. Mackenzie GG, Keen CL, Oteiza PI (2006) Microtubules are required for NF-kappaB nuclear translocation in neuroblastoma IMR-32 cells: modulation by zinc. *J Neurochem* 99:402–415.
10. Mikenberg I, Widera D, Kaus A, Kaltschmidt B, Kaltschmidt C (2007) Transcription factor NF-kappaB is transported to the nucleus via cytoplasmic dynein/dynactin motor complex in hippocampal neurons. *PLoS ONE* 2:e589.
11. Berezuk MA, Schroer TA (2007) Dynactin enhances the processivity of kinesin-2. *Traffic* 8:124–129.
12. King SJ, Schroer TA (2000) Dynactin increases the processivity of the cytoplasmic dynein motor. *Nat Cell Biol* 2:20–24.
13. Hanlon DW, Yang Z, Goldstein LS (1997) Characterization of KIFC2, a neuronal kinesin superfamily member in mouse. *Neuron* 18:439–451.
14. Bannai H, Inoue T, Nakayama T, Hattori M, Mikoshiba K (2004) Kinesin dependent, rapid, bi-directional transport of ER sub-compartment in dendrites of hippocampal neurons. *J Cell Sci* 117:163–175.
15. Jin T, Li J (2002) Dynamitin controls Beta 2 integrin avidity by modulating cytoskeletal constraint on integrin molecules. *J Biol Chem* 277:32963–32969.
16. Suzuki M, *et al.* (2004) Dynactin is involved in a checkpoint to monitor cell wall synthesis in *Saccharomyces cerevisiae*. *Nat Cell Biol* 6:861–871.
17. Cheung PY, *et al.* (2004) p150(Glued), Dynein, and microtubules are specifically required for activation of MKK3/6 and p38 MAPKs. *J Biol Chem* 279:45308–45311.
18. Kim H, *et al.* (2007) Microtubule binding by dynactin is required for microtubule organization but not cargo transport. *J Cell Biol* 176:641–651.
19. Uetake Y, Terada Y, Matuliene J, Kuriyama R (2004) Interaction of Cep135 with a p50 dynactin subunit in mammalian centrosomes. *Cell Motil Cytoskeleton* 58:53–66.
20. Meffert MK, Chang JM, Wiltgen BJ, Fanselow MS, Baltimore D (2003) NF-kappa B functions in synaptic signaling and behavior. *Nat Neurosci* 6:1072–1078.
21. Pomerantz JL, Denny EM, Baltimore D (2002) CARD11 mediates factor-specific activation of NF-kappaB by the T cell receptor complex. *EMBO J* 21:5184–5194.
22. Herman A, Croteau G, Sekaly RP, Kappler J, Marrack P (1990) HLA-DR alleles differ in their ability to present staphylococcal enterotoxins to T cells. *J Exp Med* 172:709–717.
23. Cheng HH, *et al.* (2006) Heavy chain of cytoplasmic dynein is a major component of the postsynaptic density fraction. *J Neurosci Res* 84:244–254.
24. Combs J, *et al.* (2006) Recruitment of dynein to the Jurkat immunological synapse. *Proc Natl Acad Sci USA* 103:14883–14888.
25. Ross JL, Wallace K, Shuman H, Goldman YE, Holzbaur EL (2006) Processive bidirectional motion of dynein-dynactin complexes in vitro. *Nat Cell Biol* 8:562–570.
26. Giannakakou P, *et al.* (2000) p53 is associated with cellular microtubules and is transported to the nucleus by dynein. *Nat Cell Biol* 2:709–717.
27. Harrell JM, *et al.* (2004) Evidence for glucocorticoid receptor transport on microtubules by dynein. *J Biol Chem* 279:54647–54654.
28. Carson C, Saleh M, Fung FW, Nicholson DW, Roskams AJ (2005) Axonal dynactin p150Glued transports caspase-8 to drive retrograde olfactory receptor neuron apoptosis. *J Neurosci* 25:6092–6104.
29. Moseley GW, *et al.* (2007) Dynein light chain association sequences can facilitate nuclear protein import. *Mol Biol Cell* 18:3204–3213.
30. Mesika A, Kiss V, Brumfeld V, Ghosh G, Reich Z (2005) Enhanced intracellular mobility and nuclear accumulation of DNA plasmids associated with a karyophilic protein. *Hum Gene Ther* 16:200–208.
31. Williams JC, Xie H, Hendrickson WA (2005) Crystal structure of dynein light chain TcTex-1. *J Biol Chem* 280:21981–21986.
32. Mackenzie GG, Oteiza PI (2007) Zinc and the cytoskeleton in the neuronal modulation of transcription factor NFAT. *J Cell Physiol* 210:246–256.
33. Roth DM, Moseley GW, Glover D, Pouton CW, Jans DA (2007) A microtubule-facilitated nuclear import pathway for cancer regulatory proteins. *Traffic* 8:673–686.
34. Wiegert JS, Bengtson CP, Bading H (2007) Diffusion and not active transport underlies and limits ERK1/2 synapse-to-nucleus signaling in hippocampal neurons. *J Biol Chem* 282:29621–29633.
35. Lois C, Hong EJ, Pease S, Brown EJ, Baltimore D (2002) Germline transmission and tissue-specific expression of transgenes delivered by lentiviral vectors. *Science* 295:868–872.